The 2020 World Congress on
The 2020 Structures Congress (Structures20)
25-28, August, 2020, GECE, Seoul, Korea

Vibration analysis and control of railway bridges under moving loads – a case study

*Yung-Tsang Chen[1)], Byung Gyoo Kang[2)] and Yue Chan[3)]

[1), 2)] Department of Civil Engineering, University of Nottingham, Ningbo 315100, China
[3)] Institute for Advanced Study, Shenzhen University, Shenzhen 518060, China
[1)] ytchen@gmail.com

ABSTRACT

Vibration of railway bridges due to the impact exerted by high-speed trains has been a concern in the design of these bridges. The train-induced vibration, when transmitted to the bridge foundation, may affect the nearby area where factories with vibration-sensitive manufacturing equipment may be hosted, in particular, the high-tech semiconductor industries. The vibration, if not dealt with properly, may affect the production of existing manufacturers and locales' ability to attract new companies in the high-tech sector. In this paper, a case study of a railway bridge under train's moving loads is conducted. A simply supported railway bridge representative of the railway bridges used in Taiwan high-speed rail is selected at the outset. Two types of high-speed trains, namely the Shinkanshen bullet train in Japan and the TGV train in France, are used as the moving loads on the bridge. Dynamic analysis of the bridge under moving loads in the form of analytical and finite element simulations is conducted, with a goal of examining whether the vibration is excessive under the maximum operating speed of 300 km/h. Results indicate that under maximum operating speed the dynamic response of the bridge is well under codified limits in both maximum deflection and end rotation of the bridge, and no resonance effect between the bridge and the train is observed. This paper also investigates the feasibility of adding a tuned mass damper to control the dynamic response of the bridge. Results show that the tuned mass damper can effectively reduce the vibration when the bridge resonates with the moving train.

1. INTRODUCTION

High-speed rail is a type of rail transport that runs significantly faster than traditional rail traffic; as a result, the vibration induced by a high-speed train when passing over a railway bridge is expected to be increased to a higher level as compared to regular-speed trains. The dynamic amplification related to the vertical deflection of the railway bridges

---

[1)] Associate Professor
[2)] Assistant Professor
[3)] Research Fellow

due to impact effect associated with trains' passing may be significant and could potentially affect comfort of the travelling public, service life of the bridge, as well as the habitability of the surrounding area owing to propagated bridge vibration to the ground. The train-induced ground vibration, if not dealt with properly, may affect the production of nearby existing manufacturers, particularly in the high-tech sector such as semi-conductor and liquid crystal display industries. It may also affect locales' ability to attract new companies, especially when companies in the high-tech industries are looking for sites for manufacturing, the ground borne vibration may be a major concern in their decision-making process, as the factories with vibration-sensitive equipment may be affected inevitably.

To assess the train-induced vibration of railway bridges, several vehicle-bridge-interaction models have been proposed in the literature (Liu et al. 2009, Zhang et al. 2008, Zhang et al. 2010, Salcher and Adam 2015, Yau and Fryba 2015). In most of these studies, a high-speed train is often simulated using complicated dynamic models, e.g. a car of the train is modeled as a moving mass with several springs and dash pots to represent the suspension system of the train. Both vertical and rotational responses of the train-vehicle system can also be simulated, in order to derive more precisely the dynamic response of the bridge considering its interaction with the trains. Although intensive research work has been conducted in this aspect, their application in practice is often quite limited due to the complexity in creating the analytic model and to simulate the vehicle-bridge interaction. To tackle this issue, the use of finite element method to perform analysis of the train-bridge interaction has been developed (Kwasniewski et al. 2006, Zhong et al. 2015). Finite element method uses mathematics to quantify structural behavior, wave propagation, etc., and has been widely used in solving many engineering problems. Despite its powerfulness in solving mathematical equations used to describe the physical phenomenon, the requirement for the users to understand, model, and interpret the results is quite challenging, especially for practical bridge engineers.

In this paper, a case study of a railway bridge under train's moving load is conducted. The paper uses a simple approach to model the railway bridge under high speed trains, aiming at reducing the complexity in the modeling process and obtaining promptly the bridge responses under train loads. A simply supported railway bridge representative of the railway bridges used in Taiwan high-speed rail is selected at the outset. The analytic model of a simply supported bridge under moving loads developed by Yang and Yau (1997) is adopted, with a goal of simplifying the interaction analysis and focusing on the bridge's dynamic response. Two types of high-speed trains, namely the Shinkanshen (SKS) bullet train in Japan and the TGV train in France, are used as the moving loads on the bridge. Dynamic analysis of the railway bridge under SKS and TGV trains at operating speeds are conducted. Simple finite element modeling using consistent mass beam element is also conducted, with a goal of verifying the response given by the analytic model. A tuned mass damper is attached to the mid-span of the bridge, to test the feasibility of adding such damping system to reduce the vibration induced by the high-speed trains.

2. ANALYTICAL MODEL

2.1 A simply supported bridge subjected to a moving load with constant speed

Simply supported bridges are widely used in railway systems due to several obvious advantages over continuous bridges, e.g. easy to design/construct/maintain, no consequence to the spanning beams if supporting pier sinks, no effects on bridge span if expansion/contraction due to temperature variations occurs, etc. Due to the afore-mentioned reasons, simply supported bridges are adopted by the Taiwan high-speed rail as the main structural type for short span railway bridges. Considering the great complexity of the train-bridge interaction, in the bridge model for analysis, the following assumptions are made:

1. The beam is a Euler-Bernoulli beam with a homogeneous and uniform section.
2. The mass of the train is significantly lighter than the bridge so that the inertia effect of the train can be neglected, and the train can be treated as moving loads.
3. Proportional damping of the bridge, namely the damping force is proportional to the kinetic and potential energies of the bridge, is assumed.
4. The bridge is initially at rest.

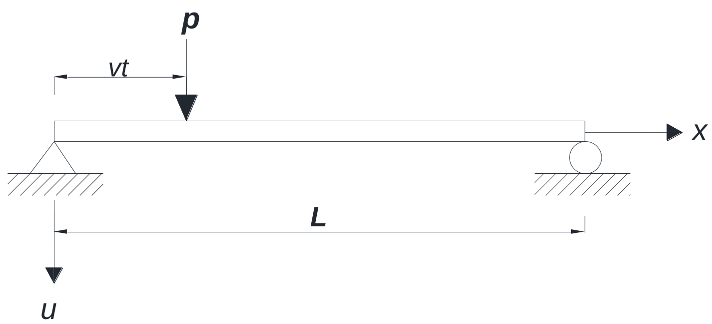

Fig. 1. A simply supported beam under a moving load with a constant speed.

When a simply supported beam bridge is subjected to a moving load p with constant speed v shown in Fig. 1., the equation of motion can be expressed as:

$$\rho A\ddot{u}(x,t) + c_e\dot{u}(x,t) + c_s I_b \dot{u}''''(x,t) + EI_b u''''(x,t) = p\delta(x - vt), 0 < vt < L \qquad (1)$$

Where $u(x,t)$ is the flexural deflection of the bridge, ρ is the density per unit length of the bridge, A is the cross-sectional area, c_e and c_s are the external and internal damping coefficients, respectively, I_b is the second moment of the area of the bridge section, E is the Young's modulus of the bridge material, p is a moving load, $\delta(\bullet)$ is the Direct Delta function, L is the bridge span, 「·」 represents taking first derivative with respect to time t, and 「′」 represents taking first derivative with respect to distance x.

Solution to Eq. (1) can be obtained using the method of separation of variables, and is listed below:

$$u(x,t) = \sum_{n=1}^{\infty} \sin\frac{n\pi x}{L} \frac{\frac{2pL^3}{EI_b\pi^4 n^4}}{(1-S_n^2)^2 + 4\xi_n^2 S_n^2}\left[(1 - S_n^2)\sin\Omega_n t - 2\xi_n S_n \cos\Omega_n t + q_n^t\right],\ 0 \le t \le \frac{L}{v}$$

$$q_n^t = e^{-\xi_n \omega_n t}[2\xi_n S_n \cos \omega_{dn} t + \frac{S_n}{\sqrt{1-\xi_n^2}}(2\,\xi_n^2 + S_n^2 - 1)\sin \omega_{dn} t \tag{2}$$

Where $S_n = \frac{\Omega_n}{\omega_n} = \frac{vL}{n\pi}\sqrt{\frac{\rho A}{EI_b}}$, is the ratio of driving frequency to the n^{th} mode Ω_n $(= \frac{n\pi v}{L})$ to the n^{th} natural frequency ω_n $(= \frac{n^2\pi^2}{L^2}\sqrt{\frac{EI_b}{\rho A}})$, ξ_n is the damping ratio of i^{th} mode, q_n^t is the transient response of the bridge, $\omega_{dn} = \omega_n\sqrt{1-\xi_n^2}$ is the damped natural frequency of the bridge.

For simply supported bridge the deflection at mid-span is usually the deflection value of concern for design. Since at mid-span ($x = \frac{L}{2}$), for second mode, forth mode, sixth mode, etc. (n=2, 4, 6…) the $\sin\frac{n\pi x}{L}$ in Eq. (2) becomes zero and mid-span can be considered a node, and since the bridge response $u(x,t)$ in Eq. (2) decays rapidly with the value of n (in n^{-4} fashion), first mode response is deemed representative of the overall bridge's response. The dynamic response of the bridge at mid-span under a moving load p with constant speed v can therefore be written as:

$$u\left(\frac{L}{2},t\right) = \frac{\frac{2pL^3}{EI_b\pi^4}}{(1-S_1^2)^2+4\xi_1^2S_1^2}[(1-S_1^2)\sin\Omega_1 t - 2\xi_1 S_1\cos\Omega_1 t + q_1^t],\ 0 \le t \le \frac{L}{v} \tag{3}$$

Since the acceleration response of the bridge is a key factor affecting the comfort of the traveling public in the trains, the acceleration response should also be obtained. The acceleration response of the bridge can be derived by taking second derivative of the displacement response $u(x,t)$ in Eq. (2) with respect to time t. Similarly, mid-span will be a node for second mode, forth mode, sixth mode, etc. (n=2, 4, 6…), if the damping of the bridge is ignored for simplicity, the acceleration response at mid-span can be expressed as:

$$\ddot{u}\left(\frac{L}{2},t\right) = \frac{2pL^3}{EI_b\pi^4}\sum_{n=1,3,5}^{\infty}\frac{\sin\frac{n\pi}{2}}{1-S_n^2}\left(\frac{\pi v\omega_n\sin\omega_n t}{n^3L} - \frac{\pi^2v^2\sin\Omega_n t}{n^2L^2}\right),0 \le t \le \frac{L}{v} \tag{4}$$

Note that to obtain the acceleration response at mid-span one can choose the first few modes but not only the first mode like the displacement response, as the acceleration response will not decays rapidly with n.

2.2 A simply supported bridge subjected to a series of moving loads

To model the loading of a high-speed train on the bridge, one may consider the train loading to be composed of a series of axle loads at constant speed v, in which the front axle in each car of the train moves at an equal spacing d, while the rear axle in each car of the train also moves at an equal spacing d, where d is the distance between two front axles in two adjacent cars as shown in Fig. 2. The distance between front and real axels of a car is L_c. If damping of the bridge is neglected for simplicity, the equation of motion for this bridge-train system can be written as:

$$\rho A\ddot{u}(x,t) + EI_b u''''(x,t) = \sum_{k=1}^{N} p[U_k(t,v,L) + U_k(t-t_c,v,L)], \tag{5}$$
$$U_k(t,v,L) = \delta[x - v(t-t_k)][H(t-t_k) - H(t-t_k-L/v)]$$

Where $t_k = (k-1)d/v$ is the time of entering the left support of the bridge, $t_c = L_c/v$ is the time difference between front and rear axles. Solution to Eq. (5) can be similarly solved using the method of separation of variables assuming boundary conditions for simply supported bridge is initially at rest, and can be expressed as:

$$u(x,t) = \frac{2pL^3}{EI_b\pi^4}\sum_{n=1}^{\infty}\frac{1}{n^4}\frac{1}{1-S_n^2}\sin\frac{n\pi x}{L}[P_n(v,t) + P_n(v,t-t_c)], \tag{6}$$
$$P_n(v,t) = \sum_{k=1}^{N}[\sin\Omega_n(t-t_k) - S_n\sin\omega_n(t-t_k)]H(t-t_k) +$$
$$(-1)^{n+1}\sum_{k=1}^{N}[\sin\Omega_n(t-t_k-L/v) - S_n\sin\omega_n(t-t_k-L/v)]H(t-t_k-L/v)$$

Where N is the number of cars that have passed the left end of the bridge.

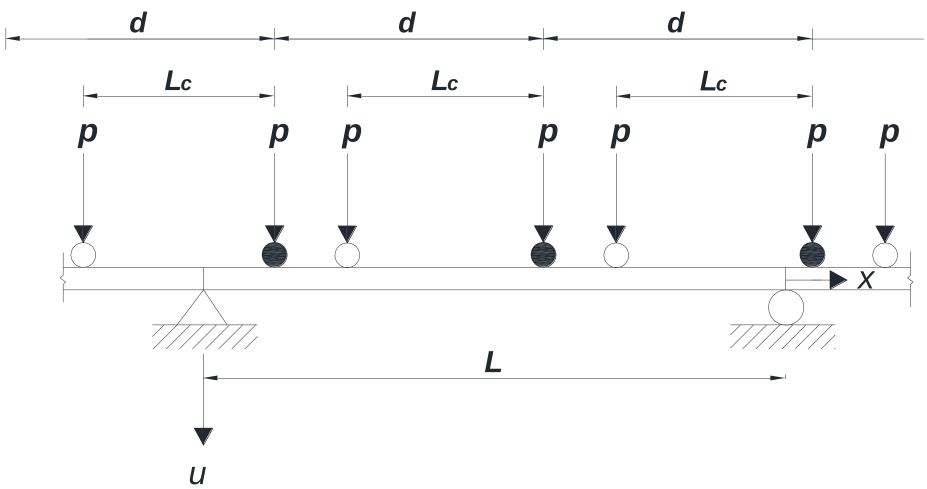

Fig. 2. A simply supported beam under a series of moving loads with constant speed.

Similarly, the displacement response of the bridge decays with n, therefore, using only first mode $(n = 1)$ to represent the overall structural response should be sufficient. If neglecting the damping ratio of the structure, the deflection at mid-span can be written as:

$$u\left(\frac{L}{2},t\right) = \frac{2pL^3}{EI_b\pi^4}\frac{1}{1-S_1^2}[P_1(v,t) + P_1(v,t-t_c)] \tag{7}$$

If end rotation is to be found, one can take first derivative of $u(x,t)$ in Eq. (6) with respect to x and plug in $x = 0$ to give:

$$u'(0,t) = \frac{2pL^3}{EI_b\pi^3}\sum_{n=1}^{\infty}\frac{1}{n^3}\frac{1}{1-S_n^2}[P_n(v,t) + P_n(v,t-t_c)] \tag{8}$$

Since in Eq. (8) the end rotation of the bridge decays with n in n^{-3} fashion, it is decided to select the first three modes of vibration to represent the overall end rotation of the bridge.

For simply supported railway bridges under train loading, due to the fact that for the bridge the nature of train is a series of constant and repeat loads, there must exists resonance and cancellation effects on the bridge. Detailed derivations for finding the train speeds causing resonance and cancelation effects on the bridge can be found in Yang and Yau (1997), and final resonance and cancellation speeds in terms of the length of a car, d, and first natural frequency of the bridge, ω_1, are listed below.

$$Resonance\ \ Speed:\ v_{res}^{(n)} = \frac{\omega_1 d}{2n\pi}, n = 1,2,3 \ldots \quad (9)$$

$$Cancellation\ \ Speed:\ v_{can}^{(n)} = \frac{\omega_1 L}{(2n-1)\pi}, \quad n = 1,2,3 \ldots \quad (10)$$

It can be observed from Eqs. (9) and (10) that when $n = 1$ both the resonance and cancellation speeds are the highest. Although not explicitly shown, the first resonance speed is the main cause of the amplified bridge deflection (Yau and Yang 2000).

3. CASE STUDY

3.1 A simply supported bridge subjected to a moving load

The approach to model the railway bridge under high speed trains can be demonstrated using a simply supported precast reinforced concrete bridge representative of the railway bridges used in Taiwan high-speed rail. Cross-section of the bridge is shown in Fig. 3. Properties of the bridge and two high-speed trains are shown in Tables 1 and 2, respectively. To verify the accuracy of the analytical procedures shown in Session 2, a moving load with constant speed is first applied, and damping ratio of the railway bridge is neglected for simplicity. Fig. 4 shows the mid-span deflection of the bridge under varied train speeds, while Fig. 5 shows the mid-span acceleration of the bridge. It can be seen from Fig. 4 that in mid-span deflection the contribution from the third mode is insignificant as compared to the first mode, thus it is reasonable to consider only first mode response. However, for mid-span acceleration the third mode cannot be neglected as its contribution in mid-span acceleration is obvious, as can be seen from Fig. 5. Fig. 6 shows the relation of the mid-span deflection with varied bridge spans and speeds of the moving load. It can be seen from Fig. 6 that with the increase of bridge span and speed, the mid-span deflection also increases, but all of them are much smaller than the allowable deflection ($\frac{u_{max}}{L} \leq \frac{1}{1600} = 0.000625$) specified in the bridge design code (Editorial Office (2004)).

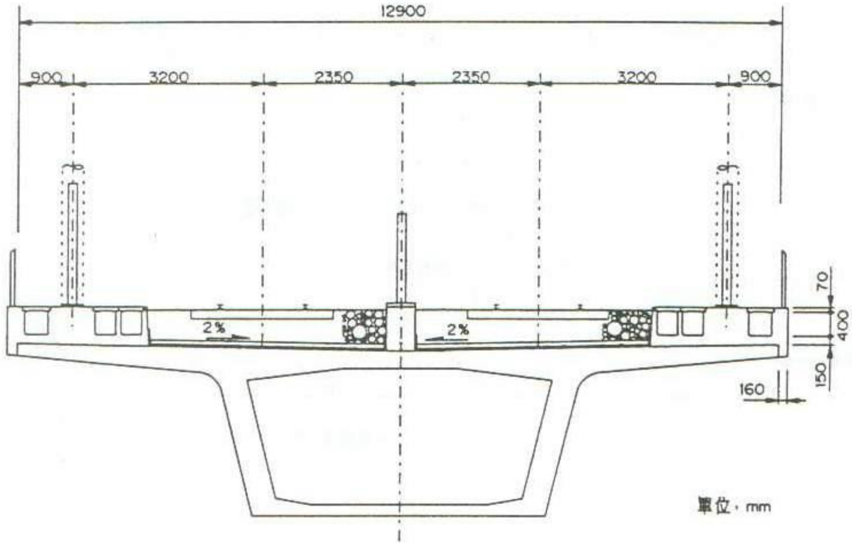

Fig. 3. Typical cross-section of high-speed railway bridges in Taiwan (Lee et al. 1998).

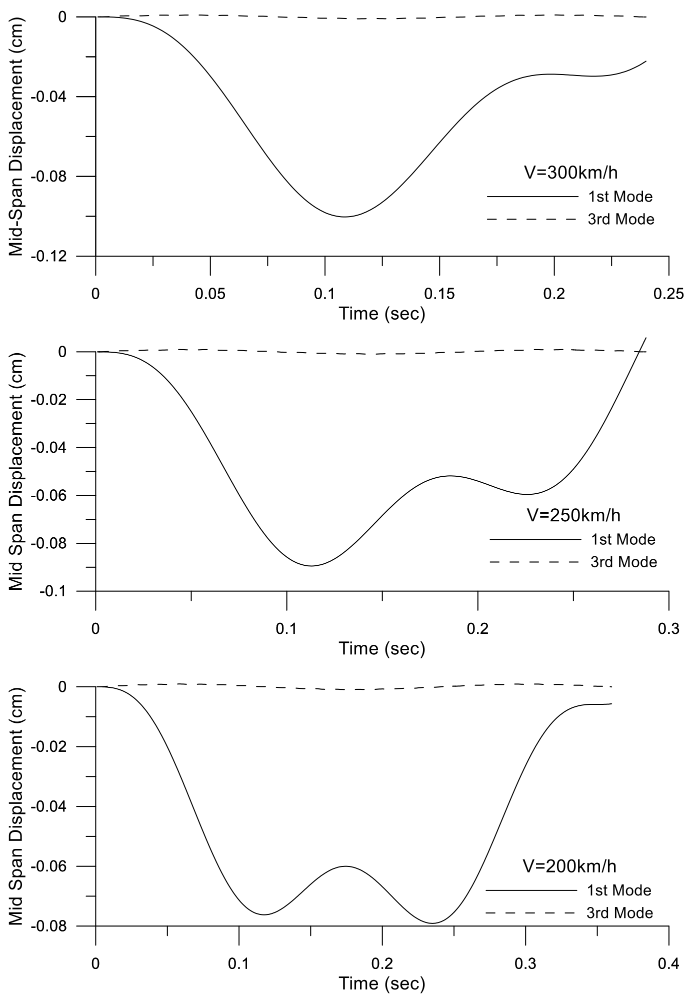

Fig. 4. Mid-span deflection of the bridge under varied train speeds.

Table 1 Properties of the high-speed railway bridge.

E (GPa)	ρ (kg/m^3)	A (m^2)	I_b (m^4)	L (m)	ω_1 (rad/sec)	p (ton)
29.43	2400	9.75	5.2	31.3	25.76	50

Table 2 Properties of TGV and SKS trains.

TGV			SKS		
p (ton)	d (m)	L_c (m)	p (ton)	d (m)	L_c (m)
16.3	21.7	18.7	24	25	17.5

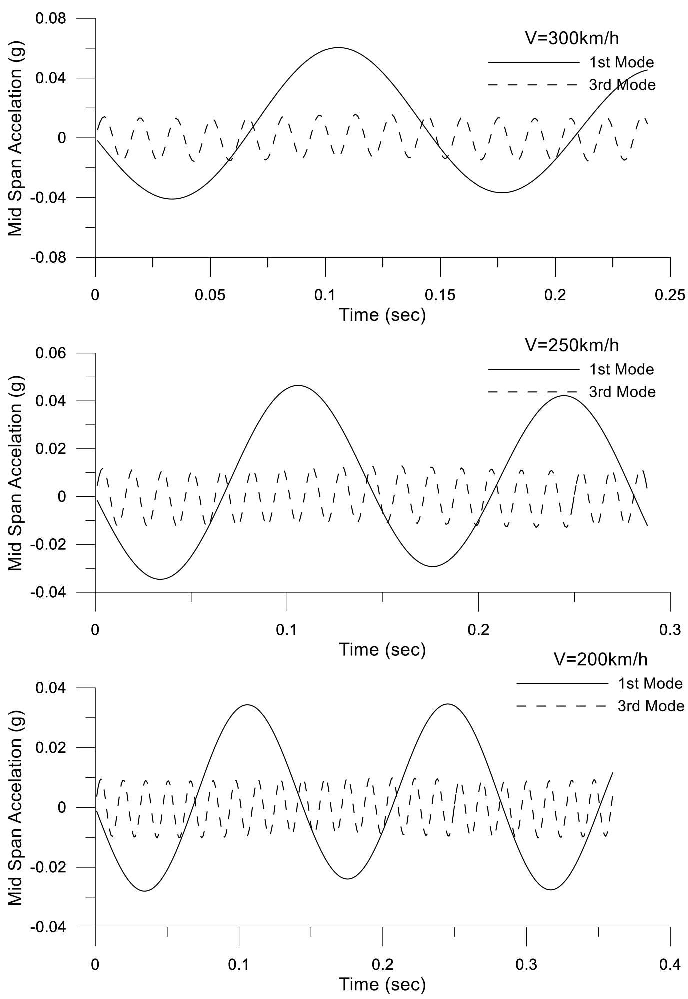

Fig. 5. Mid-span acceleration of the bridge under varied train speeds.

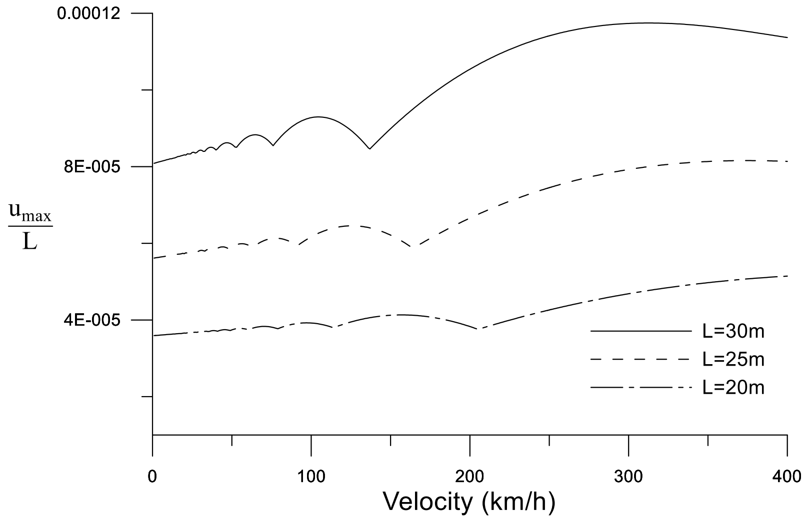

Fig. 6. Mid-span deflection of the bridge under varied bridge spans and train speeds.

3.2 A simply supported bridge subjected to train loads

The bridge is further subjected to two types of high-speed trains, namely SKS from Japan and TGV from France to test if the vibration caused by the two high speed trains is under the allowable limits specified in the codes. Fig. 7 shows the maximum mid-span deflection of the bridge with varied train speeds. It can be seen from Fig. 7 that there exist several resonance speeds for the two high speed trains. For SKS train, the first three resonance speeds are 450, 225 and 150 km/h, and the first resonance speed (450 km/h) causes the most significant bridge vibration. However, the current design bridge at maximum train operating speed (300 km/h) avoids this resonance effect. For TGV train the bridge vibration caused by the first resonance speed (336 km/h) is not obvious, which may be attributed to the fact that the first resonance speed is close to one of the cancellation speeds. Note that maximum deflection caused by either SKS or TGV trains is smaller than the allowable deflection-to-span ratio of 1/1600. It should also be noted that if the maximum deflection deflection-to-span ratio is less than 1/2800, then the check for passengers' riding comfort is not needed (Editorial Office 2004).

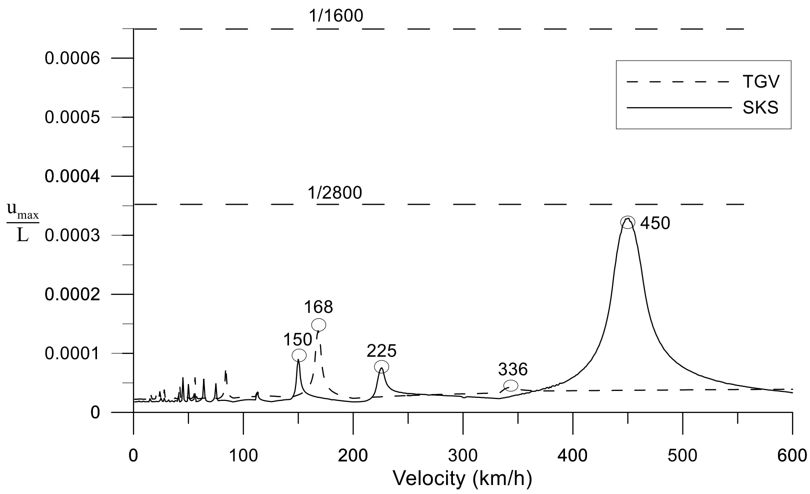

Fig. 7. Maximum mid-span deflection of the bridge with varied train speeds.

Fig. 8 shows the maximum end rotation of the bridge with varied train speeds. It can be seen from Fig. 8 that the maximum end rotation of SKS train at first resonance speed is larger than the allowable end rotation of $\frac{0.002}{h}$ $(= 0.000625)$ specified in the code (Editorial Office 2004), where h is the distance from the rail track top to the bottom of the bridge. However, the maximum operating speed of the Taiwan's high-speed rail using SKS train system is 300 km/h, thus the end rotation is well under the code-specified value. For TGV train, the largest end rotation occurs at second resonance speed, not the first one. Despite this, the maximum end rotation is still smaller than the allowable end rotation. Based on the observations made from these two cases, one can conclude that at the maximum operating speed of 300 km/h, the use of current bridge type, section, and span length is suitable for the operation of either SKS or TGV trains, in terms of safety of the bridge and comfort of the traveling public. Meanwhile, since the railway bridge is simply supported, the vibration in the bridge should not affect the joints as they are considered nodes. The impact transfer from the bridge to the ground is thus purely the axial load of the bridge column from axle loads of the high-speed trains. This impact loading is transient in nature and is close to a white noise, thus should not cause significant vibration affecting the nearby area.

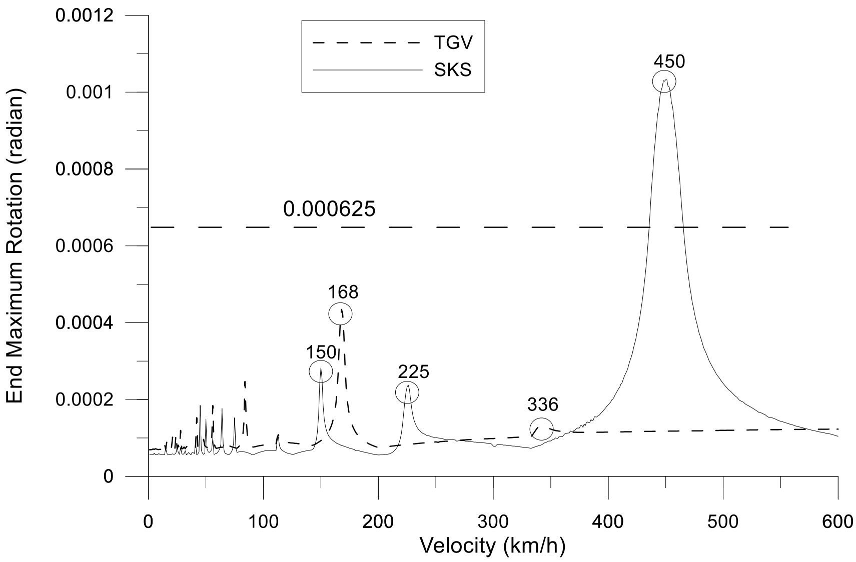

Fig. 8 Maximum end rotation of the bridge with varied train speeds.

3.3 Vibration control of the railway bridge with tuned mass dampers

Results from Section 3.2 indicate that for the current simply supported railway bridge, there is no resonance effect for both SKS and TGV trains under the maximum operating speed of 300 km/h, and the maximum deflection and end rotation are well within the allowable limits specified in the code. The comfort of the traveling public is also ensured due to the very small bridge deflection. However, we are still interested to see if the vibration of the bridge can be further reduced, especially when there is a resonant effect at second or third resonance speeds. To this end, a finite element model for the simply supported railway bridge is established. This simple model uses consistent mass and stiffness to create the bridge model. The train load is converted to equivalent loading at nodes of the beam elements in the model.

Fig. 9 shows the comparison between analytical solution and numerical simulation for TGV train with 16 cars (N=16) running at a resonant speed of 168 km/h. It can be seen from Fig. 9 that the two figures match reasonably well. The minor difference between analytical and numerical solutions is because the analytical solution considers only first mode response, while the numerical solution considers all modes of vibration of the bridge structure.

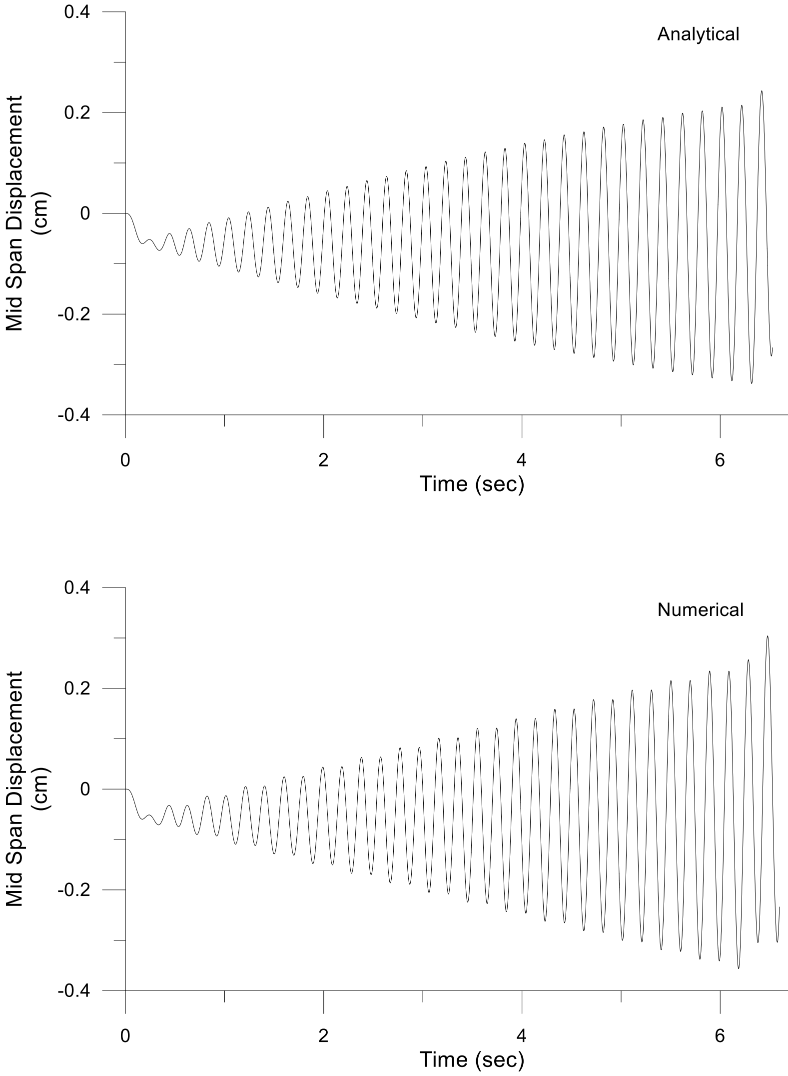

Fig. 9. Mid-span deflection of the bridge under TGV train at 168 km/h.

To test if the addition of a tuned mass damper can effectively reduce the bridge vibration due to high-speed trains, a tuned mass damper is installed in the middle of the bridge span inside the bridge cell to control its vertical deflection. The tuned mass damper is installed at the mid-span because mid-span has the largest vibration. The tuned mass damper has a mass ratio (mass of the tuned mass damper to that of the railway bridge) of 1%, with optimized spring stiffness k_d and damping coefficient c_d as shown in Table 3. The corresponding frequency ratio and damping ratio of the damper are also listed in Table 3. The optimal damper parameters are obtained from a gradient based optimal search (Lee et. al 2006) assuming white noise input and 1% mass ratio.

Table 3 Optimal design parameters of the tuned mass damper.

Damper mass m_d (ton)	Damping coefficient c_d $(kN.s\ /m\ )$	Stiffness coefficient k_d $(kN\ /m\ )$	Mass ratio μ $(= m_d/m_s)$	Frequency ratio f $(= f_d/f_s)$	Damping ratio ξ_d $(=\frac{c_d}{2m_d\omega_d})$
7.32	27.3	4.93	1%	0.9857	7.19%

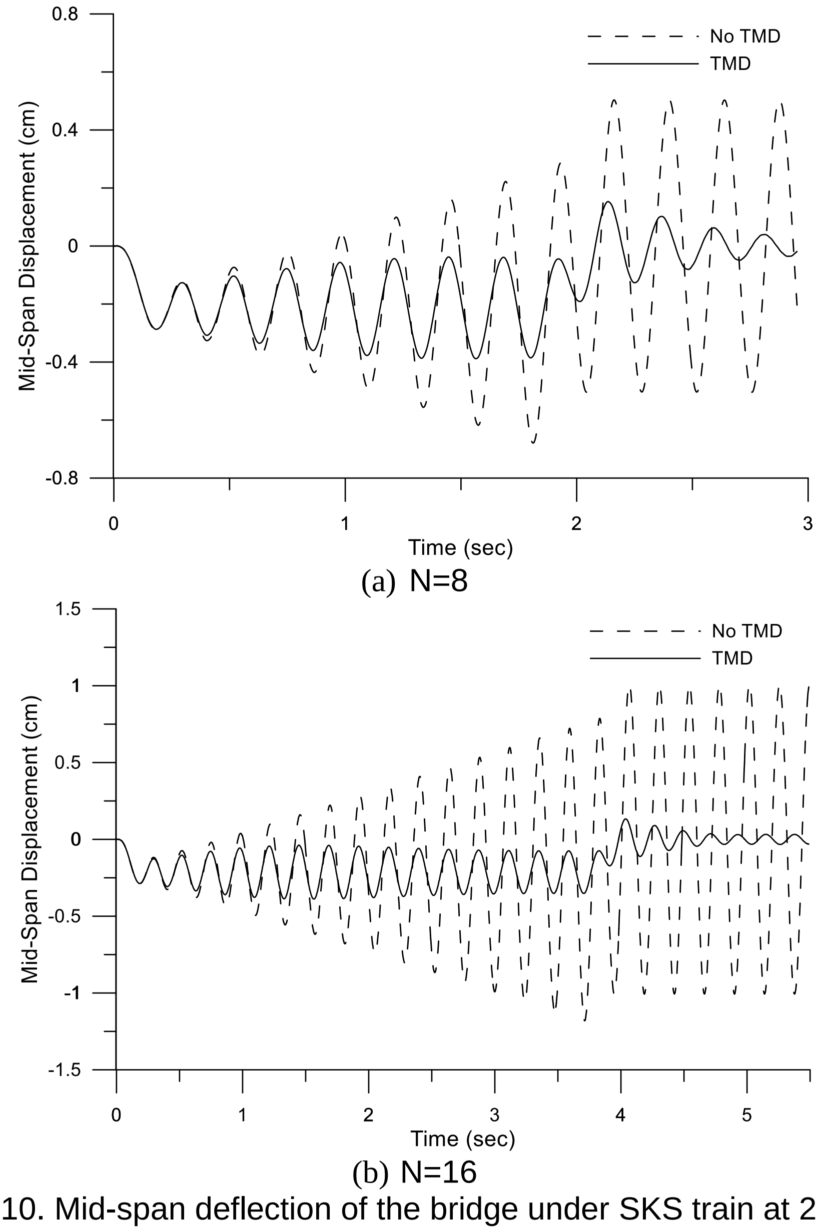

Fig. 10. Mid-span deflection of the bridge under SKS train at 266 km/h.

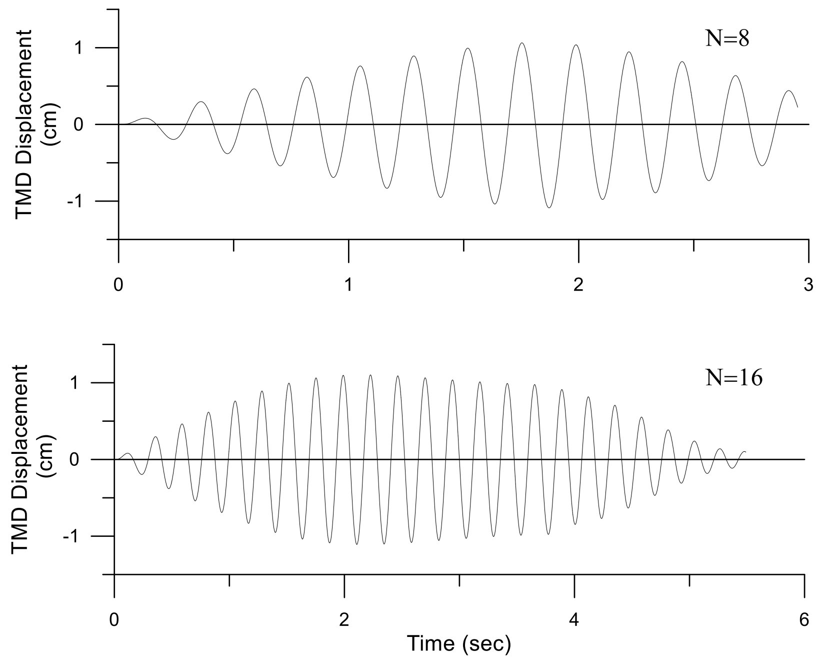

Fig. 11. Displacement of the tuned mass damper installed at the railway bridge.

Fig. 10 shows the mid-span deflection of the bridge under SKS train at a resonance speed of 266 km/h. It can be seen from Fig. 10 that the bridge resonates with the train as the train is operated at resonance speed, and the bridge deflection increases with increasing number of cars (N) of the train. With the installation of a tuned mass damper at mid-span, the deflection response is reduced significantly. Although the maximum operating speed of 300 km/h is not a resonant speed for the current train (SKS) and bridge configuration, it may be useful if bridge vibration is a concern for other types of train-bridge assembly, or the train is operated near the resonance speeds. Fig. 11 shows the displacement time history of the tuned mass damper. It can be seen from Fig. 11 that the displacement of the tuned mass damper is relatively small, in both N=8 and N=16 cases. This is an important characteristic since the space inside the bridge cell is usually confined, which makes tuned mass dampers quite suitable for railway bridge applications. The tuned mass damper is therefore considered a feasible and effective damper device for suppressing bridge vibration caused by high-speed trains.

4. CONCLUSION

In this paper, a case study of a railway bridge under train's moving load is conducted. The paper uses a simple approach to model the railway bridge under high speed trains, aiming at reducing the complexity in the modeling process and obtaining promptly the bridge responses under train loads. Dynamic analysis of a representative simply supported railway bridge under SKS and TGV trains at varied speeds are conducted. Simple finite element modeling using consistent mass beam element is also conducted, with a goal of verifying the response given by the analytic model. Results from the simple model indicated that the bridge response can be readily obtained with sufficient accuracy, and at current maximum operating speed of 300 km/h, bridge vibration caused by either SKS and TGV trains are well within the acceptable limits and no resonance effect is observed. A tuned mass damper is attached to the mid-span of the bridge to test the feasibility of adding such damping system to reduce the vibration induced by high-speed trains. Results indicate that the installation of an optimized tuned mass damper can reduce the bridge vibration effectively when the bridge resonates with the train.

ACKNOWLEDGEMENTS

We gratefully acknowledge the financial support from the Faculty Inspiration Grant.

REFERENCES

Editorial Office (2004), *Design code for railway bridges*, Ministry of Transportation and Communication, Taipei, Taiwan.

Kwasniewski, L., Li, H., Wekezer, J. and Malachowski, F. (2006), "Finite element analysis of vehicle-bridge interaction", *Finite Elements in Analysis and Design*, **42**(22), 950-959.

Lee, C.L., Chen, Y.T., Chung L.L. and Wang, Y.P. (2006), "Optimal design theories and applications of tuned mass dampers", *Engineering Structures*, **28**, 43-53.

Lee, Y.S., Hwang, F.J. and Zheng, S.H. (1998), *Design parameters and analysis of vertical vibration and longitudinal forces of railway bridges for high-speed trains.* R-ST-98-02, Sinotech Engineering Consultant, Taipei, Taiwan.

Liu, K., De Roeck, G. and Lombaert, G. (2009), "The effect of dynamic train-bridge interaction on the bridge response during a train passage", *Journal of Sound and Vibration*, **325**, 240–251.

Salcher, P. and Adam, C. (2015), "Modeling of dynamic train–bridge interaction in high-speed railways", *Acta Mechanica*, **226**, 2473–2495.

Yang, Y.B. and Yau, J.D. (1997), "Vehicle-bridge Interaction element for dynamic analysis," *Journal of Structural Engineering, ASCE,* **123**, 1512–1518.

Yau, J.D. and Fryba, L. (2015), "A quasi-vehicle/bridge interaction model for high speed railways", *Journal of Mechanics,* **31**(2), 217-225.

Yan, J.D. and Yang, Y.B. (2000), *Theory of high-speed train-bridge interaction*, Zetech, Taipei, Taiwan.

Zhang, N., Xia, H. and Guo, W.W. (2008), "Vehicle-bridge interaction analysis under high speed trains", *Journal of Sound and Vibration*, **309**, 407–425.

Zhang N., Xia H., Guo W.W., De Roeck G. (2010), "A vehicle–bridge linear interaction model and its validation", *International Journal of Structural Stability and Dynamics*, **10**(2), 335–361.

Zhong, H., Yang, M. and Gao, Z. (2015), "Dynamic responses of prestressed bridge and vehicle through bridge-vehicle interaction analysis", *Engineering Structures*, **87**, 116-125.